ACOUSTIC TOMOGRAPHY FOR DECAY DETECTION IN BLACK CHERRY TREES[1]

Xiping Wang*†

Senior Research Associate
Natural Resources Research Institute
University of Minnesota Duluth
and
USDA Forest Service, Forest Products Laboratory
1 Gifford Pinchot Drive
Madison, WI 53726-2398

Jan Wiedenbeck†

Project Leader
USDA Forest Service
Northern Research Station
241 Mercer Springs Road
Princeton, WV 24740

Shanqing Liang

PhD Candidate
Research Institute of Wood Industry
Chinese Academy of Forestry
Xiangshan Road
Beijing, China 100091

Abstract. This study investigated the potential of using acoustic tomography for detecting internal decay in high-value hardwood trees in the forest. Twelve black cherry (*Prunus serotina*) trees that had a wide range of physical characteristics were tested in a stand of second-growth hardwoods in Kane, PA, using a PiCUS® Sonic Tomograph tool. The trees were felled after the field test and a disc from each sampling height was cut and subjected to laboratory evaluations. It was found that acoustic tomography underestimates heartwood decay when it is the major structural defect in the trees. However, when an internal crack is present in the tree trunk, the acoustic tomography tends to overestimate the size of the defects. In the presence of ring shake in the cross-section, the acoustic shadows resemble the influence of both extensive heartwood decay and lateral cracks. These findings highlight the importance of determining the nature of structural defects when assessing hardwood trees using the acoustic tomography technique. Results from this study offer insights that may be used to improve the interpretation algorithm embedded in the tomography software.

Keywords: Acoustic tomography, decay, defect, hardness, hardwood trees.

INTRODUCTION

Internal decay in standing timbers causes the U.S. wood industry to spend millions of dollars to process and reprocess wood so that decayed portions are not included in products. It is estimated that for all the timber harvested annually in the United States, heartwood decay fungi destroy about 30% of the timber volume. Heartwood decay is thought to cause more than twice as much timber volume loss as all other hardwood and conifer diseases combined (Tainter and Baker 1996).

The economic loss caused by heartwood decay is most significant for the hardwood trees that are

---

* Corresponding author: xwang@fs.fed.us
† SWST member

used to produce appearance-grade veneer products. The veneer logs cut from these trees typically cost 1.5 – 6 times the value of Forest Service Grade 1 sawlogs (Wiedenbeck et al 2004). Because of the exceptionally high prices paid for veneer-quality trees, undetected decay can cause a substantial monetary loss to timber buyers and veneer manufacturers. The loss includes not only the purchase price, but also log shipping and handling costs, expense of log storage, and costs associated with log processing up to the point when the defect is discovered. Early detection of internal decay in hardwoods could provide a significant benefit to the industry in terms of making accurate quality assessments and volume estimates and use of the resource. It can also help foresters in prescribing silvicultural treatments for improved management decision-making and thus help maintain a healthy forest.

In recent years, tomography techniques that were developed for engineering and medical applications have been evaluated for their applicability in standing trees. Investigations on urban trees showed great success using tomography to detect internal decay hidden from view within the trunks. Nicolotti et al (2003) applied three different types of tomography (electric, ultrasonic, and georadar) to urban trees with different degrees of success. Of the three technologies, ultrasonic tomography proved to be the most effective tool for detecting internal decay, locating the position of the anomalies and estimating their sizes and shapes. Gilbert and Smiley (2004) evaluated an acoustic tomography tool for its ability to quantify decay in white oak (*Quercus alba*) and hickory (*Carya* spp.). They reported a high correlation between the amount of decay detected by the tomograms and that actually present in the cross-section ($r^2 = 0.94$). The average accuracy for samples in which decay was present was 89%. One important fact that needs to be noted is that internal cracks, a common defect in many hardwood trees, was not present in the trees they evaluated. Similarly, a recent investigation on century-old red oak trees at the Capitol Park in Madison, WI, also showed great success in using the

acoustic-type tomography technique to detect internal structural defects (Wang et al 2007a, 2007b).

So far, laboratory investigation and field application of acoustic tomography have been largely focused on urban trees with the principal goal being to determine the stability of the trees to minimize the risk of tree failure. The potential of this technology for assessing the quality of high-value hardwood trees in production forests has not been fully investigated (Wang et al 2005).

The objectives of this study were to assess the probability and reliability of the acoustic tomography technique for detecting internal decay in high-value black cherry trees in the forest and to determine how structural defects other than decay (such as internal cracks and ring shake) might affect tomographic results and interpretation.

MATERIALS AND METHODS

Tree Selection

The sample site was located just south of Kane, PA, in McKean County and was part of the Collins Pennsylvania Forest. The black cherry (*Prunus serotina*) trees that we selected were located in a stand of second-growth Allegheny hardwoods slated for harvest in 2007. The forests of the Allegheny Plateau are widely recognized for the quality of the black cherry timber that grows there. More than one-third of the cherry veneer logs sold in world markets originate from these forests (Allegheny National Forest 2002). Tree selection procedures involved two steps: initial screening and final sample tree selection. The goal of the procedure was to obtain trees with different levels of internal decay. For comparison purposes, healthy trees were also included in the experimental plan.

We first preselected 20 black cherry trees through visual examination and application of a single-path stress wave test. These 20 trees were labeled and assigned a tracking number. The diameter at breast height was measured and a stress-wave test was conducted in two perpendicular directions at breast height. These preselected trees had a wide range of physical conditions in terms of

physiological characteristics and stress wave transmission times. From these 20 trees, we then selected 12 sample trees for the main purpose of this study. The visual grades of the 12 were: Forest Service Tree Grade 1 (4), Grade 2 (3), Grade 3 (4), and below grade (1).

Field Acoustic Tomography Test

All 12 black cherry trees were first nondestructively tested using a multichannel acoustic measurement system—PiCUS® Sonic Tomograph (Argus Electronic Gmbh, Rostock, Germany). Figure 1 shows the application of a PiCUS Sonic Tomograph tool in testing black cherry trees in the forest.

The PiCUS® Sonic Tomograph measurement system consisted of 12 sensors, which were evenly placed around the trunk in a horizontal plane. Each sensor was magnetically attached to a pin that was tapped into the bark and sapwood. Acoustic wave transmission times were measured by sequentially tapping each pin using the steel hammer. A complete data matrix was obtained through this measurement process at each location. Figure 2 shows the sensor arrangement and the paths of acoustic measurements for the test.

The sample trees were first tested at a height of about 50 cm above the ground. When potential

internal decay or defects were identified in the acoustic tomogram at this height, two more tests were then conducted at successively greater heights up the trunk, 100 and 150 cm. At each height, the circumference and distances between sensors were measured using a tape and a PiCUS® caliper. This information was used as an input for the system software to map the approximate geometric form of the cross-sections. On completion of acoustic measurements, a tomogram was constructed for each cross-section using the PiCUS® Q70 software.

During testing, each test height on all sample trees was marked and the pins for sensors 1 and 7 were marked so that they could be traced back to the original location in the tree.

After acoustic tomography tests were completed, the sample trees were felled and a 5 cm thick disc was cut from each test height. This sample disc was subsequently labeled with tree number and height (eg 1 – 50). A digital picture of the cross-section was then taken on all freshly cut sample discs. A total of 20 discs were obtained in the field. All discs were placed in plastic bags and taken back to the laboratory for further evaluation.

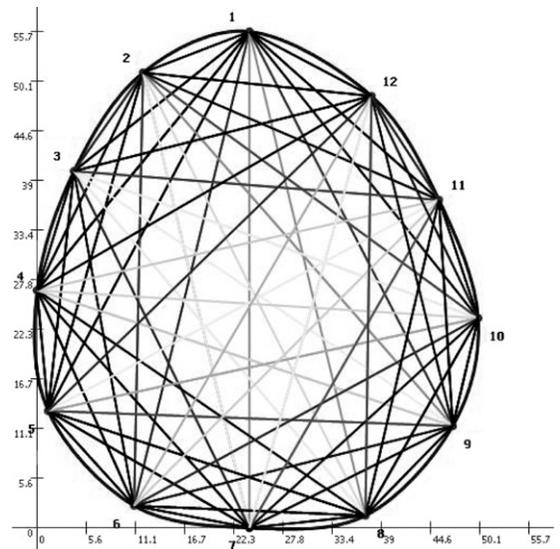Figure 1. Acoustic tomography test on black cherry trees using a Picus® Sonic Tomograph tool.

Figure 2. Sensor arrangement and paths of acoustic measurement.

Laboratory Evaluation

Visual examination. Freshly cut discs were first shipped to the Forestry Sciences Laboratory in Princeton, WV, for visual examination. The 20 sample discs were carefully surfaced and physically examined for internal conditions in terms of discoloration and severity and location of decay. The criteria used for assessing the severity of decay condition are as follows:

Decay: very soft wood but still in place; and

Incipient decay: soft wood with open pores but hard to mark with fingernails.

Hardness test. After visual examination at the Princeton laboratory, the sample discs were shipped to the Forest Products Laboratory in Madison, WI, for further physical and mechanical tests. In the laboratory, all disc samples were conditioned to 12% EMC in an environment of 24°C and 66% RH. Seven discs having a range of internal physical conditions were selected to develop hardness maps of the cross-sections. Before conducting hardness tests, the disc samples were marked with 25×25 mm grids on the top surfaces. The vertical grids on the discs were aligned north to south and the horizontal grids east to west (Fig 3).

The end hardness of the disc samples was obtained using the Janka ball hardness test procedure given in ASTM D 143-94 (ASTM 2005). The hardness test was conducted on each grid cell using indentation on the cross-sectional face.
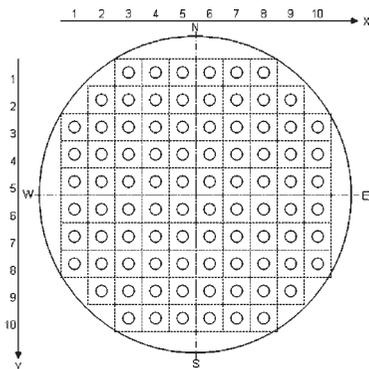

Figure 3.   Schematic of hardness mapping grids.

The test setup (Instron testing machine [Instron Corporation, Norwood, MA]   with a standard 11.28 mm dia steel ball mounted on the crosshead) allowed continuous recording of load as a function of the penetration depth of the steel ball into the wood. A threshold was set to automatically record the "maximum load" at an indentation of 5.64 mm as specified in ASTM D143-94.

Data Analysis

The goals of data analysis were to determine: (1) if the acoustic tomograms generated from the black cherry trees matched the internal decay and other structural defects on the cross-sections; (2) how internal wood defects other than decay affect the tomogram and its implications for tomogram interpretation; and (3) the degree of accuracy and reliability of acoustic tomography in detecting heartwood decay and other defects in black cherry trees.

Acoustic wave transmission data obtained from acoustic measurements on sampled trees were used to generate the 2D velocity distribution (tomogram) using PiCUS® software for each sampling height. Acoustic tomograms of the trees were generated in predesignated color scheme (Argus Electronic Gmbh 2006): brown (dark brown/light brown), green, and violet/blue/white, with dark brown representing the high acoustic velocity, high density, and sound wood; violet/blue/white representing areas of low velocity, low density, and unsound wood; and green the transition zone (barrier wall) between deteriorated and sound wood. The color scale is expanded between the 100% and lowest velocity.

In principle, an acoustic tomogram shows the distribution of acoustic velocity in a cross-section of a tree, where acoustic measurements are conducted. The color presentation of acoustic velocity zones demonstrates the differences in the ability of the wood to transmit acoustic waves. The ability of the wood to transmit acoustic signals within a cross-section strongly correlates with its modulus of elasticity and density (Bucur 2003). Therefore, the tomogram can be

interpreted as a "modulus map" or "density map" of the cross-section.

The end hardness values obtained from the selected discs were used to determine the distribution of hardness in the cross-sections. Both 2D and 3D hardness maps were created for each black cherry disc using Matlab software (The Mathworks, Inc., Natick, MA).

RESULTS AND DISCUSSION

Table 1 summarizes the findings of both tomography testing on the trees and laboratory visual assessment of the discs. Of 12 black cherry trees acoustically tested, five (trees 1, 2, 4, 18, and 19) were predicted to have severe internal defects, and seven (trees 7, 10, 11, 12, 15, 16, and 17) were predicted to be sound and healthy. The tomogram-based diagnoses were all confirmed by visual assessment of the discs (Table 1).

Laboratory examination of the discs indicated that black cherry trees diagnosed as defect positive had several different types of structural defects, including heartwood decay, sapwood decay, internal cracks, and ring shake. Although the acoustic tomography does not identify the types of structural defects within a tree, such information seemed to be associated with the shapes of the acoustic shadows and how the colors are spread across the tomogram.

Acoustic Tomogram vs Photographic Image

Heartwood decay. The structural defects found in tree 1 were the most significant of all tested trees with both tomograms and disc images confirming heartwood decay at all three heights. Laboratory examination confirmed the presence of brown-rot decay fungus. The tomograms of tree 1 at 50, 100, and 150 cm heights

Table 1. *Acoustic shadows and internal defects revealed in the black cherry trees.*

| Tree no. | Elevation (cm) | Cross-section diameter (cm) | Acoustic shadow[a] (%) | | Defects revealed in disc and estimated decay area | Tomography diagnosis |
			VBW[b]	VBWG[c]		
1	50	54.5	20	32	Decay: 24%; incipient decay: 14%; total: 38%	Positive
	100	50.6	17	26	Decay: 25%; incipient decay: 7%; total: 32%	Positive
	150	49	10	26	Decay: 9.4%; incipient decay: 10.6%; total: 20%	Positive
2	50	42.4	29	40	Lateral crack extended from sapwood to center	Positive
4	50	56.1	35	54	Ring shake	Positive
	100	53.5	2	17	Ring shake not fully developed; one-third separation	Positive
	150	52.5	0	0	Very early stage of ring shake development; no separation	Positive
7	50	54.8	0	0	Mostly clear	Positive
10	50	55.4	0	0	Mostly clear	Positive
11	50	41.7	0	0	Clear	Positive
12	50	34.4	0	0	Mostly clear; small warm hole near sapwood	Positive
15	50	49.7	0	0	Clear	Positive
16	50	64.3	0	0	Clear	Positive
17	50	42	0	0	Clear	Positive
18	50	54.1	12	27	Lateral crack all way through cross-section	Positive
	100	51.6	17	32	Lateral crack all way through cross-section	Positive
	150	50.3	22	37	Lateral crack all way through cross-section	Positive
19	50	59.9	24	47	Lateral crack through pith; small decay pocket at sapwood	Positive
	100	58	23	38	Major lateral crack; small decay pocket on sapwood	Positive
	150	57.3	30	40	Multiple radial cracks; small decay pocket on sapwood	Positive

[a] Area with green, violet, blue, and white colors.
[b] VBW = violet, blue, and white colors.
[c] GVBW = green, violet, blue, and white colors.

(a) Cross-section No. 1-50

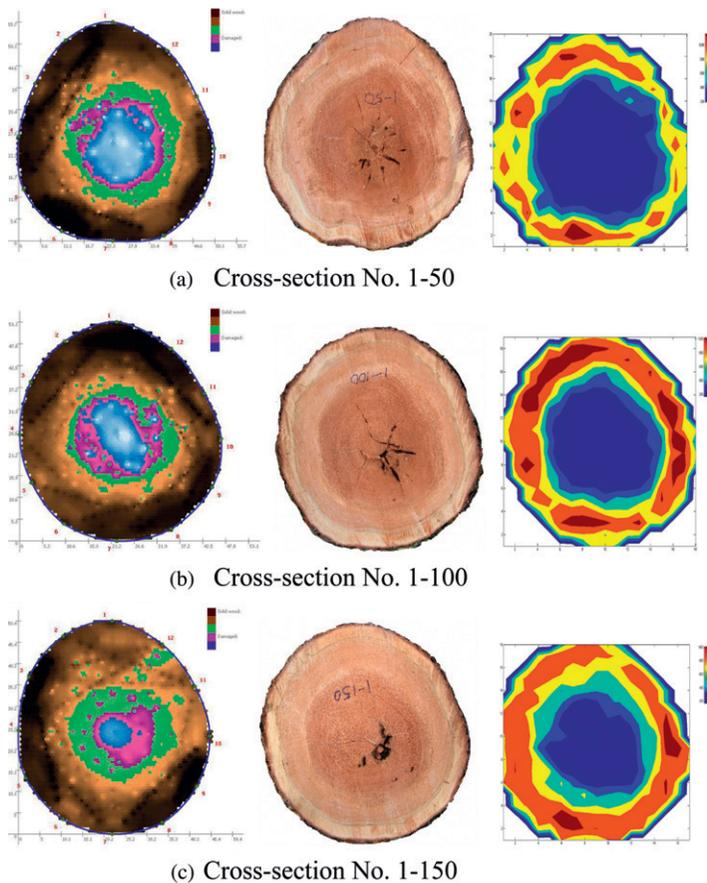(b) Cross-section No. 1-100

(c) Cross-section No. 1-150

Figure 4.   Acoustic tomograms vs photographic images and 2D hardness maps of the discs (tree 1: heartwood decay).

showed large acoustic shadows in the central areas of the cross-sections (Fig 4, images on the left). The shape of the shadows was close to a round form. The size of the shadow was the largest at the lower height (50 cm) and decreased progressively as the height above ground increased. The acoustic shadows (green, violet, blue, and white) at the three sample heights were 36, 26, and 26% of the total cross-sectional area. The more severely damaged areas, as indicated by violet, blue, and white colors, were 20, 17, and 10%, respectively. Visual examination of the discs revealed significant heartwood decay at the same locations with acoustic shadows (Fig 4, images in the middle). The estimated total decay areas (decay and incipient decay) were 38, 32, and 20%

of the cross-section at the three heights. The estimated severe decay areas were 24, 25, and 9% of the cross-section at three heights. It is evident that the acoustic shadows in the tomograms are generally in good agreement with the physical conditions revealed by visual examination of the discs.

Internal cracks. Tomograms of trees 2, 18, and 19 contain large bands of acoustic shadows, which expand across almost the entire diameter in two cases [Fig 5(a – b), discs 2 – 50 and 18 – 100] and across two-thirds of the diameter in the other case [Fig 5(c), disc 19 – 150]. The total areas of the acoustic shadows were 40, 27 – 37, and 38 – 47% of the cross-sectional area for trees 2, 18, and 19, respectively. Visual

examination of the discs revealed large lateral cracks (discs 2 – 50, 18 – 50, 18 – 100, and 18 – 150) and a combination of lateral cracks and radial cracks (discs 19 – 50, 19 – 100, and 19 – 150) as dominating structural defects. These cracks, largely in the radial direction and extended up and down in vertical planes within the trunk, effectively cut off linear propagation of the acoustic waves diverting them to a much longer travel path. The direct result of this was that, even without significant decay present, the software produced a wide band of acoustic shadow in the tomograms. This observation was consistent with warnings provided in the operating manual (Argus Electronic Gmbh 2006).

Ring shake. The tomogram of tree 4 at 50 cm height showed that 54% of the cross-sectional area was covered by acoustic shadows [Fig 5(d)]. The shape of the shadow was nearly round, which could indicate severe heartwood decay damage. However, visual examination of the disc indicted that the major defect was ring shake, not heartwood decay. In this case, the ring shake acted as a major crack that cut off linear propagation of the acoustic waves. As a result of the geometric nature of the ring shake (round), the acoustic shadow produced by the software resembled the influence of both extensive heartwood decay and internal cracks.

Visual examination of the discs for tree 4 further indicated that early stages of ring shake extended up to 100 and 150 cm heights but showed no clear separation of the wood fibers. These early stages were not identified by the tomograms.

Sound wood and minor defects. Tomograms of trees 7, 10, 11, 12, 15, 16, and 17 showed no acoustic shadows in the cross-section. The visual examination of the discs revealed that the cross-sections were mostly clear and sound wood, which confirmed the acoustic diagnosis. As an example, Fig 5(e) shows the tomogram and photographic image of the corresponding disc for a sound cross-section.

(a) Cross-section No. 2-50

(b) Cross-section No. 18-100

(c) Cross-section No. 19-150
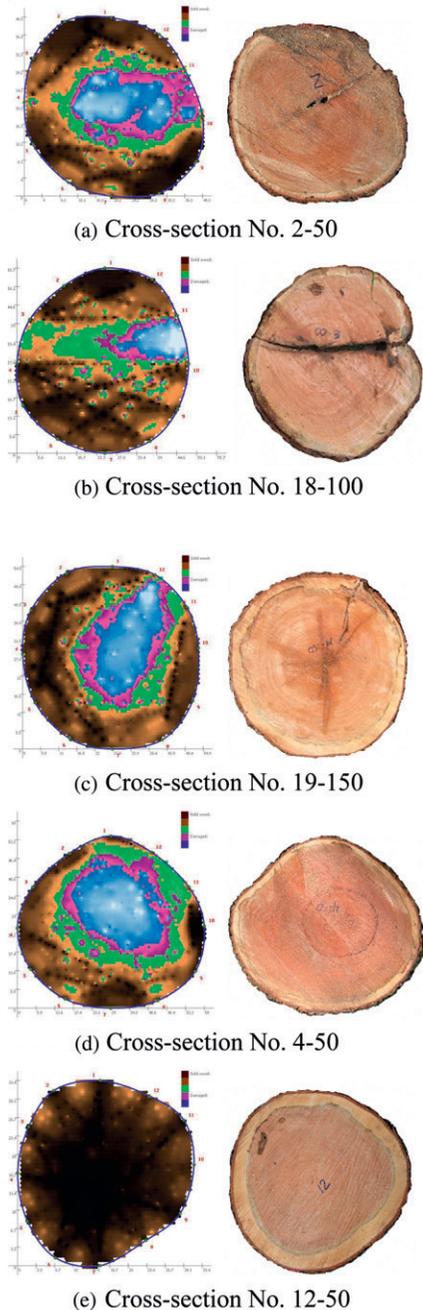
(d) Cross-section No. 4-50

(e) Cross-section No. 12-50

Figure 5. Acoustic tomograms vs photographic images of the discs (trees 2, 18, and 19: internal crack; tree 4: ring shake; tree 12: sound wood with minor defects).

Some minor defects such as small decay pockets (heartwood and sapwood decay) and worm holes were present in trees 7, 12, 15, and 17

(less than 1% of the cross-section). These were not detected in the tomograms as a result of the limited resolution of the equipment.

Acoustic Tomogram vs Hardness Map

As a result of time constraints, hardness measurements were only conducted on seven discs: 1 – 50, 1 – 100, 1 – 150, 2 – 50, 12 – 50, 17 – 50, and 18 – 50. These discs were selected because they had a range of structural defects (decay, incipient decay, lateral cracks) and therefore were deemed to be good representatives of the disc samples.

Table 2 shows the end-hardness values of both heartwood and sapwood for the seven selected discs. Table 3 shows the areas of acoustic shadows and internal decay as revealed by hardness maps.

Cross-sections with sound wood. To accurately interpret the cross-sectional maps of end hardness, we need to understand the normal range of values of end hardness as it occurs across the cross-sections of the sound discs. Of seven selected discs for hardness mapping, discs 12 – 50 and

17 – 50 were the clearest samples having only minor defects (small insect holes, less than 1% of the cross-sectional area). We used these two as examples of sound discs and excluded the hardness values of the small defective spots in data analysis. Figure 6 shows the 3D hardness maps of the two sound discs (12 – 50 and 17 – 50). The distribution of hardness is relatively flat in the heartwood zones. Analysis of hardness values indicated that end hardness of heartwood is significantly higher than that of sapwood. In the case of these two sound discs, the hardness of heartwood ranged from 4500 – 6316 N for disc 12 – 50 and 4506 – 7184 N for disc 17 – 50. The hardness of sapwood was 3034 – 4724 N for disc 12 – 50 and 3523 – 5653 N for disc 17 – 50, which was 29 and 23% lower than that of heartwood, respectively. This implies that when assessing the hardness maps of the cross-sections, the hardness values should be interpreted relative to the radial zone (ie heartwood vs sapwood).

Cross-sections with heartwood decay. Figure 7 shows the 3D hardness maps of the three cross-sections in tree 1 that had significant

Table 2. *End-hardness values of the black cherry discs.*

	End hardness (N)						
	Sapwood			Heartwood			
Disc no.	Minimum	Maximum	Average	Minimum	Maximum	Average	Physical condition
12 – 50	3033	4725	3809	4500	6314	5385	Sound
17 – 50	3523	5655	4627	4504	7183	6006	Sound
1 – 50	2805	4337	3581	0	6023	2344	Heartwood decay
1 – 100	2277	4321	3446	0	5276	2677	Heartwood decay
1 – 150	2599	4089	3216	0	5242	2872	Heartwood decay
2 – 50	N/A	N/A	N/A	0	5352	3715	Lateral crack
18 – 100	1810	4396	3205	0	6511	4353	Lateral crack, sapwood decay

N/A, not available.

Table 3. *Acoustic shadows and internal defects reveled by hardness maps.*

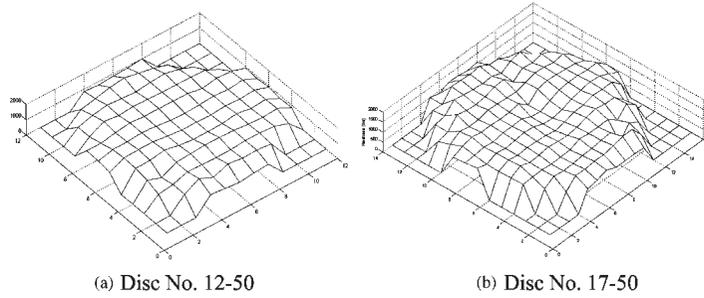|		Acoustic shadow (%)			Hardness mapping (%)		
Tree no.	Elevation (cm)	Violet, blue, and white (moderate to severe decay)	Green (incipient decay)	Total	Decay	Incipient decay	Total
12	50	0	0	0	0	0.9	0.9
17	50	0	0	0	0.6	0	0.6
1	50	20	12	32	33.3	12.9	46.2
	100	17	9	26	28.3	15.1	43.4
	150	10	16	26	20.2	18.3	38.5
2	50	29	11	40	6	9.8	15.8
18	100	17	15	32	8.6	5.1	13.7

(a) Disc No. 12-50   (b) Disc No. 17-50

Figure 6.   3D hardness maps of sound discs (trees 12 and 17).

(a) Disc No. 1-50
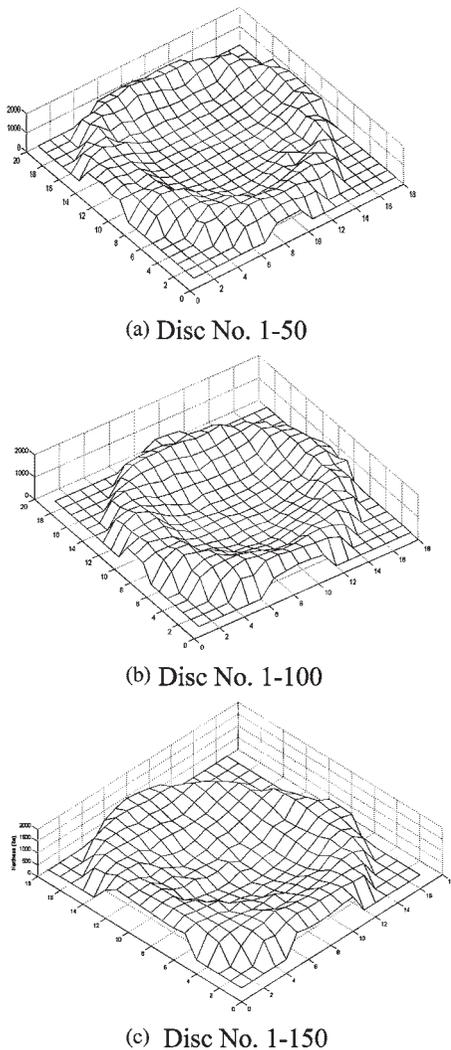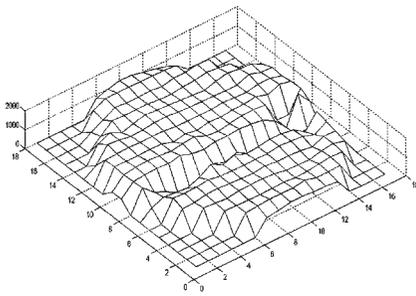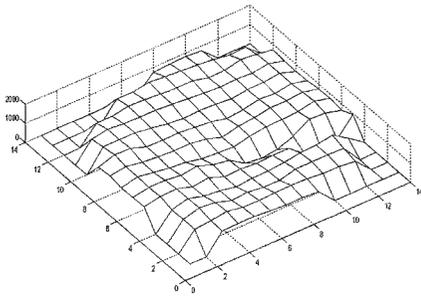

(b) Disc No. 1-100

(c) Disc No. 1-150

Figure 7.   3D hardness maps of discs with heartwood decay (tree 1).

heartwood decay. Compared with the relatively flat 3D hardness maps of the sound discs in Fig 6, the 3D hardness maps of these cross-sections (1 – 50, 1 – 100, and 1 – 150) exhibited a large area of depression in the heartwood zone, which represents significant heartwood decay at all three sample heights. When comparing the 3D hardness maps with the acoustic tomograms, we found that the percentage area of heartwood decay in the cross-sections apparently exceeded the size of the acoustic shadows in the tomogram (Table 3), suggesting the prediction by acoustic tomography underestimates this defect. Conversely, the 3D hardness mapping results may help redefine the boundary of acoustic shadows in tomography and improve the precision. In the case of discs 1 – 50, 1 – 100, and 1 – 150 in which substantial heartwood decay was present, the light brown color in the tomogram seems to correspond to the incipient decay zones in the cross-sections and therefore should not be treated as sound wood.

Cross-sections with internal cracks. Figure 8 shows the 3D hardness maps of the cross-sections that had internal cracks (discs 2 – 50 and 18 – 100). Hardness analysis indicated that lateral cracks are the major structural defects in these two discs, but there was also some incipient decay associated with the cracks. The lateral cracks in the discs are well reflected in the 3D hardness maps as shown in Fig 8. When comparing the 3D hardness maps with the acoustic tomograms, we found that the areas of acoustic shadows in the tomograms are significantly

(a) Disc No. 18-100

(b) Disc No. 2-50

Figure 8.   3D hardness maps of discs with lateral cracks (trees 2 and 18).

larger than the defect areas mapped by hardness. This indicated that acoustic tomography tends to overestimate the size of defect when a crack is present in the cross-sections, which is the reverse of the phenomena associated with heartwood decay. This highlights the importance of determining the nature of structural defects when assessing standing trees using acoustic tomography.

The hardness distribution of the cross-sections can also be illustrated using 2D color maps as shown in Fig 4 (images on the right). The color scale for the maps is shown in the upper-right side of each figure. In general, dark blue represents very low hardness values and dark red very high hardness values with transition colors between the low and high hardness values. For example, in the case of 2D hardness maps of three cross-sections in tree 1, dark blue and blue indicate severe to moderate decay and light blue indicates incipient decay. It should be noted that the blue color on the periphery does not represent any defects, but simply a mathematical

treatment to form the boundary of the cross-sections. By comparing the 2D hardness maps with the acoustic tomograms, we can observe the differences between areas of acoustic shadows and the blue color areas of the hardness maps. We now know that the hardness map can serve as a better calibration model than visual assessment of the discs in assessing the accuracy and precision of acoustic tomography.

SUMMARY AND CONCLUSIONS

Twelve trees that had a wide range of physical characteristics were evaluated in a stand of second-growth black cherry using acoustic tomography. The trees were felled after a field acoustic tomography test and a disc was cut from each sampling height. The discs were visually examined for internal conditions and then mechanically tested across a cellular grid to map the end hardness of the cross-sections. The acoustic tomograms of the trees were evaluated by comparing them with the photographic images and hardness maps of the cross-sections. Based on the data analysis, we conclude the following:

1. Acoustic tomography is capable of detecting various internal structural defects in black cherry trees, including heartwood decay, internal cracks, and ring shake. The nature of the structural defects is associated with the shapes of the acoustic shadows and how the colors are distributed across the tomogram.
2. When heartwood decay is the major structural defect in trees, the prediction of decay areas by acoustic tomography is underestimated. The acoustic shadows (violet, blue, and white colors) are significantly smaller than the true decay areas as indicated by hardness maps. Our analysis suggests that the light brown areas in the tomogram are likely associated with incipient decay in the cross-section and therefore cannot be simply treated as sound wood.
3. When internal cracks are present in the cross-section, acoustic tomography tends to

overestimate the size of the defect. The acoustic shadows are usually in the form of a wide band and its size is significantly greater than the true defect area as indicated by the hardness maps. This highlights the importance of determining the nature of structural defects when assessing trees using acoustic tomography techniques.

4. When ring shake is present in the cross-section, the acoustic shadows resemble the influence of both extensive heartwood decay and lateral cracks. The size of acoustic shadows far exceeds the diameter of the ring shake. In this case, additional evidence by visual observation or microdrilling is needed to differentiate between heartwood decay and ring shake-induced acoustic shadows.

5. Acoustic tomography cannot reliably detect small sapwood decay and insect holes in mostly sound cross-sections.

Although acoustic tomography has the capability to detect heartwood decay and other major defects in high-value hardwood trees, application of current commercial acoustic tomography devices seems limited. This is primarily because the testing process of such commercial tools is time-consuming and not cost-effective. The implementation of such technology in the field for anything other than the highest value trees (eg historic or exceptionally large urban trees) requires significant change in equipment design and improvement in the interpretation software. Results from this study should provide insights on possible changes to the tomography software that might enhance its applicability for field use.

REFERENCES

Allegheny National Forest (2002) Master interpretive plan. USDA Forest Service. Eastern Region. 15 pp.

Argus Electronic Gmbh (2006) PiCUS® Sonic Tomograph manual. Rostock, Germany.

ASTM (2005) Standard methods of testing small clear specimens of timber. D 143-94. American Society for Testing and Materials, West Conshohocken, PA.

Bucur V (2003) Nondestructive characterization and imaging of wood. Springer-Verlag, Berlin, Heidelberg, Germany. 354 pp.

Gilbert EA, Smiley ET (2004) PiCUS Sonic Tomography for the quantification of decay in white oak (*Quercus Alba*) and hickory (*Carya* spp.). J Arboric 30(5):277 – 280.

Nicolotti G, Socco LV, Martinis R, Godio A, Sambuelli L (2003) Application and comparison of three tomographic techniques for detection of decay in trees. J Arboric 29:66 – 78.

Tainter FH, Baker FA (1996) Principles of forest pathology. John Wiley & Sons, New York, NY. 803 pp.

Wang X, Wiedenbeck J, Ross RJ, Forsman JW, Erickson JR, Pilon C, Brashaw BK (2005) Nondestructive evaluation of incipient decay in hardwood logs. Gen. Tech. Rep. FPL-GTR-162. USDA Forest Service, Forest Products Laboratory. 11 pp.

———, Allison RB, Wang L, and Ross RJ (2007a) Acoustic tomography for decay detection in red oak trees. Research Paper FPL-RP-642. USDA Forest Service, Forest Products Laboratory, Madison, WI. 7 pp.

———, ——— (2007b) Decay detection in red oak trees using a combination of visual inspection, acoustic testing, and resistance microdrilling. J Arboric Urban For 34(1):1 – 4.

Wiedenbeck J, Wiemann M, Alderman D, Baumgras J, Luppold W (2004) Defining hardwood veneer log quality attribute. Gen. Tech. Rep. NE-313. USDA Forest Service, Northeastern Research Station. 36 pp.